ELSEVIER

Journal of Molecular Structure 567–568 (2001) 319–338

Journal of
MOLECULAR
STRUCTURE

www.elsevier.nl/locate/molstruc

Inter- and intramolecular O–H···π hydrogen bonding in the methanol–ethene complex and *syn*-7-norbornenol, probed by IR, ^{1}H NMR and quantum chemistry ☆

Leif H. Bjerkeseth[a,*], Jan M. Bakke[a], Einar Uggerud[b]

[a]*Organic Chemistry Laboratories, Norwegian University of Science and Technology, N-7491 Trondheim, Norway*
[b]*Department of Chemistry, University of Oslo, P.O. Box 1033 Blindern, N-0315 Oslo, Norway*

Received 6 July 2000; accepted 19 September 2000

Abstract

The geometries and energies of *syn*-7-norbornenol (**1**) have been investigated with theoretical and experimental methods, while its epimer *anti*-7-norbornenol (**2**) has been investigated by theoretical methods only. It was found that **1** is intramolecularly hydrogen bonded and exists almost exclusively in its hydrogen bonded form, the *Anti* conformer. Compound **2**, for which intramolecular hydrogen bonding is impossible, was found to exist as the *Gauche* conformer. A theoretical investigation of the model complex between methanol and ethene showed that the interaction energy is -3.1 ± 0.1 kcal mol^{-1} (estimated Hartree–Fock basis set limit plus correlation contribution, not including vibrational zero point energy). Electron correlation is essential in the evaluation of the interaction energy and also for the geometry of the complex. It was found that the potential energy surface around the minimum energy structure is flat, with an almost freely rotating methanol part.

Keywords: *Syn*-7-Norbornenol; Methanol–ethene complex; Intermolecular hydrogen bonding; Intramolecular hydrogen bonding; Hydrogen bonding

1. Introduction

The idea of the classical hydrogen bond was first suggested 80 years ago by Latimer and Rodebush [1]. However, the phenomenon did not really reach common acceptance until Pauling in 1939 published the first edition of 'The Nature of the Chemical Bond' [2], in which the hydrogen bond was considered to be mainly an electrostatic ('ionic') interaction. A broader definition was later given by Pimentel and McClellan in 1960 [3], expanding it to A–H···A′ where A and A′ not necessarily are electronegative atoms [4]. Hydrogen bonds where A or A′ are ionic are among the strongest, while hydrogen bonds of the type X–H···A, where the acceptor A is an electronegative atom and X is e.g. C, N or O, are termed normal or weak [5]. At the end of the 1950s and in the 1960s, π-systems like a carbon–carbon double or triple bond or an aromatic ring also became recognised as hydrogen bond acceptors (non-classical hydrogen bond) [6,7]. In recent years, the observation of X–H···π hydrogen bonds has become rather frequent [5].

☆ Dedicated to Professor Marit Trætteberg on the occasion of her 70th birthday.

* Corresponding author. Present address: Forsvarets forsknings-institutt, Norwegian Defence Research Establishment, Division for Protection and Materiel, P.O. Box 25, N-2027 Kjeller, Norway. Tel.: +47-63-80-78-97; fax: +47-63-80-75-09.

E-mail address: Leif-Haldor.Bjerkeseth@ffi.no (L.H. Bjerkeseth).

0022-2860/01/$ - see front matter
PII: S0022-2860(01)00563-4

Table 1
IR spectroscopic data for *syn*-7-norbornenol (**1**) and *anti*-7-norbornenol (**2**) in the OH stretch region. All spectra recorded at high dilution in CCl_4 (tetrachloroethylene for Ref. [30], solvent not given for Ref. [27]). Numbers in parentheses are band half widths

Frequencies/cm^{-1}			Band areas[a]/(%)			Ref.
ν_1	ν_2	ν_3	ν_1	ν_2	ν_3	
Syn-7-Norbornenol (**1**)						
3572						[27]
3624	3574					[28,29]
3575						[30]
3628 (31)	3575 (22)		18	82		[31]
3628 (25)	3590[b] (18)	3575 (17)	18	9[b]	73	Present study[b]
3628 (25)	3575 (17)		20	80		Present study, corrected
Anti-7-Norbornenol (2)						
3628						[27]
3630						[28,29]
3632 (27)						[31]

[a] Integrated absorptions.
[b] 88% pure **1**. Recorded at c < 5 mM in CCl_4. Band 2 was caused by an unidentified impurity.

We have previously studied the conformation of several unsaturated alcohols and other compounds with a geometrical possibility for an intramolecular O–H···π or O–H···F hydrogen bond, and have discussed the importance of intramolecular hydrogen bonding [3–10] for the conformational composition for such compounds [11–17]. The investigations were performed by a combination of theoretical calculations and IR and ^{1}H NMR spectroscopy. The combination of experiment and theory is necessary to fully understand the conformational behaviour in molecules like these.

Hydrogen bonded complexes are fundamentally important for understanding the nature of the hydrogen bond phenomenon [18]. The geometry/directionality of the hydrogen bond is less well defined for the O–H···π hydrogen bond than for stronger hydrogen bonds. We, therefore, considered it to be of interest to investigate this point from both a theoretical and experimental point of view:

By studying the *inter*molecular case, where the hydroxyl group is completely free to move relative to the double bond. For this purpose the 1:1 methanol–ethene complex was chosen.
By studying the *intra*molecular case, where the hydroxyl group has the opportunity to interact with the double bond. For this purpose the homoallylic *syn*-7-norbornenol (**1**) is ideal. In **1**, the hydroxyl group is, from visual inspection of models, in constant close proximity to the double bond and has a unique geometrical possibility for an intramolecular hydrogen bond. Its OH-epimer *anti*-7-norbornenol (**2**) will be used as a reference since this cannot form an O–H···π bond.

To our knowledge, no information about a 1:1 methanol–ethene complex has been published until now. However, several papers describing the analogous 1:1 water–ethene complex [16,19–26] have been published.

Compounds **1** and **2** have been the subject of a number of investigations by IR [27–32], ^{1}H NMR [32,33], MS (EI ionisation energy) [34], photoelectron spectroscopy [30], CNDO/2 [35] and ab initio molecular orbital calculations (HF/STO-3G) [36]. The question of intramolecular O–H···π hydrogen bonding [3–10] has been central to these studies. Only one band was reported for **2** in the hydroxyl stretch region in the IR spectrum [27–29,31,32] while both one [27,30,32] and two [28,29,31] bands (bands 1 and 2) have been reported for **1** (Table 1). However, two bands were reported for **1** in all the papers focusing primarily on infrared spectroscopy [28,29,31]. The band for **2** had approximately the same frequency as band 1 for **1** while band 2 for **1**

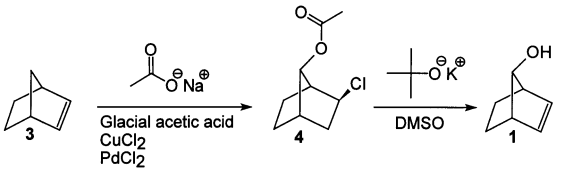

Fig. 1. Synthesis of *syn*-7-norbornenol (**1**).

appeared at a 53 cm^{-1} lower frequency, indicating that **1** was intramolecularly hydrogen bonded.

2. Synthesis

Syn-7-Norbornenol (**1**) was prepared from norbornene (**3**) in a two-step synthesis as shown in Fig. 1. Exo-2-chloro-*syn*-7-acetoxynorbornane (**4**) was first prepared by heating norbornene (**3**) with sodium acetate and copper (II) chloride in glacial acetic acid using a catalytic amount of palladium (II) chloride as described by Baird [37]. Further reaction with potassium *tert*-butoxide in DMSO as described by Baird [37] gave *syn*-7-norbornenol (**1**).

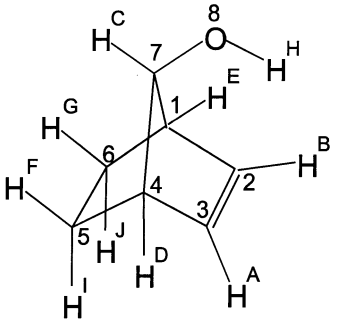

1

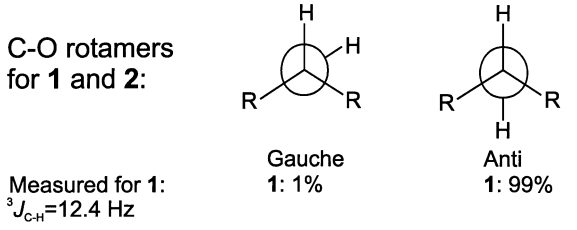

Fig. 2. Notations for *syn*-7-norbornenol (**1**) and Newman projections of the C–O rotamers of *syn*-7-norbornenol (**1**) and *anti*-7-norbornenol (**2**). Conformational composition of **1** from ^{1}H NMR.

3. Experimental

3.1. Materials

Syn-7-Norbornenol (**1**) prepared according to the procedure above was recrystallised and sublimed to 88% purity (GC, DB-1). The most abundant by-product (unknown) constituted 4% of the remaining 12%. The spectroscopic data were in accordance with those previously reported [32,38–41].

3.2. ^{1}H NMR

The ^{1}H NMR spectrum of **1** was recorded at high dilution at room temperature in CCl_3F on a Bruker AM 500 spectrometer, using a sealed capillary tube with deuterated benzene for locking purposes. Chemical shifts are reported as ppm relative to TMS. The CCl_3F solvent was distilled from freshly activated 3 Å molecular sieves and kept over activated 3 Å molecular sieves in a cold room. The high dilution CCl_3F solution for NMR ($c < 5$ mM) was prepared in the NMR tube in the cold room and was kept over freshly activated 3 Å molecular sieves for some days before measurement.

^{1}H NMR (500 MHz): δ 0.86–0.98 (2H, m, $H^{I,J}$), 1.55 (1H, d, $J_{C-H} = 12.40$ Hz, H^H), 1.64–1.76 (2H, m, $H^{F,G}$), 2.65–2.70 (2H, m, $H^{D,E}$), 3.63 (1H, d, $J_{C-H} = 12.35$ Hz, H^C), 6.00–6.04 (2H, m, $H^{A,B}$). J_{C-H} denotes the $^3J_{H-H}$ coupling constant between H^C and H^H. For notation, see Fig. 2.

3.3. IR

The IR spectrum of **1** was recorded at high dilution ($c < 5$ mM) at room temperature in CCl_4 on a single beam Nicolet 20SXC FT-IR spectrometer equipped with a Nicolet 620 Data Station and a TGS detector using IR quartz cells with 10 mm path length (transparent in the hydroxyl stretch frequency region in IR), 256 scans and 2 cm^{-1} resolution. The instrument was purged with dry air. The CCl_4 solvent was refluxed over and subsequently distilled from P_2O_5 under N_2 atmosphere and kept over activated 3 Å molecular sieves in a dry box under N_2 atmosphere. The high dilution CCl_4 solution for IR was prepared and added to the IR cells in the dry box, and was kept over freshly activated 3 Å molecular

Table 2
Calculated conformer populations (%) for *syn*-7-norbornenol (**1**) and *anti*-7-norbornenol (**2**)

Method (full geometry optimisation)	*Syn*-7-Norbornenol			*Anti*-7-Norbornenol	
	Gauche	*Anti*	$^3J_{CH-OH}$/(Hz)[a]	*Gauche*	*Anti*
MMPMI	84	16	3.85	97	3
MMPMI[b]	35	65	8.90	86	14
MMX87	71	29	5.19		
MMX87[b]	52	48	7.14		
MNDO	52	48	7.14	88	12
AM1	–[c]	100		2	98
PM3	–[c]	100		–[c]	100
HF/STO-3G	12	88[d]	11.3		
HF/3-21G	0	100[e]	12.5	96[f]	4
HF/6-31G**	2	98[g]	12.3	95[h]	5
HF/6-31++G**	2	98[i]	12.3	95[j]	5
HF/6-31++G(2d,2p)	2	98[k]	12.3	94[l]	6
MP2(FU)/6-31G**	1	99[m]	12.4	90[n]	10
MP2(FU)/6-31++G**[o]	1	99[p]	12.4	91[q]	9
^{1}H NMR[r]	1[a]	99[a]	12.4[r]		

[a] Calculated from $J = 2.2X_{Gauche} + 12.5X_{Anti}$ and $X_{Gauche} + X_{Anti} = 1$, where X is the molecular fraction; see Section 4.1.1.
[b] Charge-charge interaction modus.
[c] No *Gauche* minimum was found.
[d] The electronic energy is −341.4939650 hartrees.
[e] The electronic energy is −343.8076868 hartrees.
[f] The electronic energy is −343.8069393 hartrees.
[g] The electronic energy is −345.7356505 hartrees.
[h] The electronic energy is −345.7367080 hartrees.
[i] The electronic energy is −345.7442254 hartrees.
[j] The electronic energy is −345.7454643 hartrees.
[k] The electronic energy is −345.7574337 hartrees.
[l] The electronic energy is −345.7584139 hartrees.
[m] The electronic energy is −346.9235650 hartrees.
[n] The electronic energy is −346.9244697 hartrees.
[o] Optimised without second analytical derivatives.
[p] The electronic energy is −346.9467910 hartrees.
[q] The electronic energy is −346.9481449 hartrees.
[r] Experimental data.

sieves for 24 h before measurement. Overlapping bands were resolved by the FOCAS 2.1 program from Nicolet using a linear baseline approach. The number of bands and their positions were assessed by use of Fourier self deconvolution (FSD). No constraints were applied to band positions, band widths, band intensities and the percent Gaussian:Lorentzian band shape during the curve-fitting process.

Note: Keeping a dilute solution over activated molecular sieves will reduce the concentration and make it impossible to measure absolute values of integrated absorptions. However, relative values are valid.

3.4. Theoretical calculations

Molecular mechanics calculations were performed on a PC with the programs MMPMI 1.0 [42] or MMX 87.200 using the default dipole–dipole electrostatic mode, or, where noted, charge–charge interaction mode. MMPMI consists of MM2 (N.L. Allinger, QCPE Program no. 395) and MMP1 (N.L. Allinger, QCPE Program no. 318) as implemented by Serena Software, Bloomington, Indiana, USA. MMX 87.200 consists of another implementation of MM2 (QCPE Program no. 395) and MMP1 (QCPE Program no. 318). Input files were made on a PC using PCMODEL

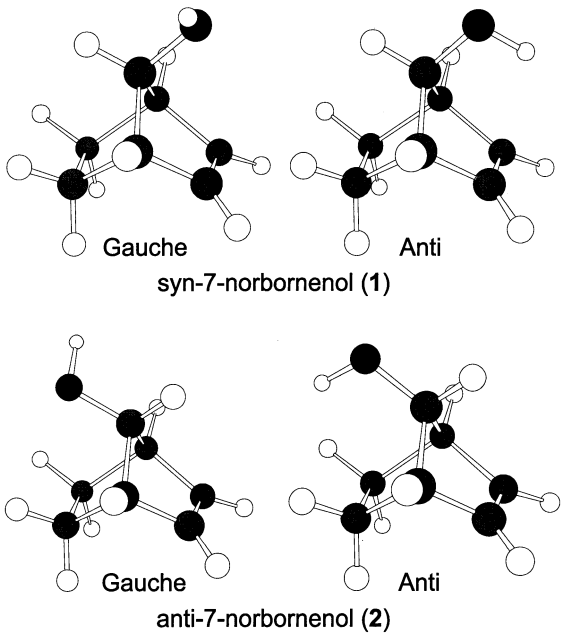

Fig. 3. Three-dimensional view of the ab initio (MP2(FU)/6-31++G**) minimum energy structures of the *Gauche* and *Anti* conformers of *syn*-7-norbornenol (**1**) and *anti*-7-norbornenol (**2**).

version 1.0 or 4.0 from Serena Software. The individual point charges for MMPMI in charge–charge mode were calculated with CHARGE2, version 1.0 [43–47] on a PC.

The semiempirical MNDO, AM1 and PM3 molecular orbital calculations were performed with MOPAC 6.00 [48] on a Digital Vaxstation 3100 M38. Input files were made by PCMODEL.

Ab initio molecular orbital calculations were performed with GAUSSIAN 90, Revision I [49], with GAUSSIAN 92, revision C or G.2 [50], or with GAUSSIAN 94, revision B.1 or D.4 [51], on the Cray X-MP/216, Cray Y-MP4D/464, Cray J916/8128 and Cray T3E supercomputers in Trondheim. The calculations were done using either the Hartree–Fock (HF) method or Møller–Plesset perturbation theory to second order (MP2 [52]). A large variety of standard basis sets implemented in GAUSSIAN were used, as indicated in Section 4 below, using standard notation. We note especially Dunning's correlation consistent basis sets with and without augmented functions (cc-pVxZ and aug-cc-pVxZ, where x = D, T, Q) [53–55]. Input files were made by PCMODEL or by hand. Tight SCF convergence criteria (as implemented in GAUSSIAN) was used for all calculations. Whether the MP2 calculations were done with frozen core (FC) or including the core electrons (FU) is evident from Tables 2 and 6. For all the MP2 calculations with Pople's basis sets, the core electrons were included. Geometries were gradient optimised using the Berny optimiser and default GAUSSIAN convergence criteria. Analytical second derivatives were computed in the final stage of all geometry optimisations except where noted in Tables 2 and 6. Analytical second derivatives were also calculated for all hydroxyl stretch frequency calculations. All vibrational frequencies for all calculated conformers of the 7-norbornenol series were positive, confirming that the stationary points were all local minima. The calculations on the 7-norbornenol series were done without symmetry restrictions. The geometries of the methanol–ethene complex (C_s) and its components methanol (C_s) and ethene (D_{2h}) were optimised within the indicated point groups. The geometries of the components of the complex were allowed to vary freely. Calculation of the basis set superposition error (BSSE) [56,57] were done using the counterpoise method [58] as described by Frisch et al. [59]. To estimate the BSSE of the proton acceptor, we added basis functions for methanol to the optimised geometry of ethene. For the estimation of the BSSE of the proton donor, we added basis functions for ethene to the optimised geometry of methanol. The location of the additional functions was determined from the geometry of the methanol–ethene complex at the same level of theory.

The conformational compositions were calculated from the relative energies, using the Boltzmann's law of distribution at 298 K. For the ab initio molecular orbital calculations, the compositions were calculated based on total energy (electron energy) with no correction for vibrational zero point energy.

4. Results and discussion

*4.1. Syn-7-Norbornenol (**1**)*

We have recently studied the conformational composition of the simplest homoallylic alcohol, 3-buten-1-ol (**5**), by IR, ^{1}H NMR and theoretical calculations [17]. This molecule has also been studied by

electron diffraction by Trætteberg et al. [60] and by microwave spectroscopy by Møllendal et al. [61]. Only two conformers of **5** have, by visual inspection of models, a geometrical possibility for intramolecular hydrogen bonding. These two conformers were denoted Conformer **12** and Conformer **13**. Our investigations showed that Conformer **13** was the only hydrogen-bonded conformer and that Conformer **12** was hardly populated. One of the models used for Conformer **12** was the homoallylic alcohol 3-cyclopenten-1-ol (**6**) which was found to exist predominately with the OH-group in an axial position. However, no indication of intramolecular hydrogen bonding in **6** was found. For Conformer **13**, epicholesterol (**7**) was used as a model. **7** was found to be intramolecularly hydrogen bonded.

The 3-cyclopenten-1-ol skeleton can be considered being built into *syn*-7-norbornenol (**1**) (Fig. 3) and thus forced into a rigid conformation with the OH-group in an axial position. From visual inspection of models, the rigid structure in **1** causes a decrease in the C–C–C bond angles in the 3-cyclopenten-1-ol skeleton, thus decreasing the distances between the proton acceptor and proton donor functions, and thereby forcing the hydroxyl group and the double bond to interact.

In *syn*-7-norbornenol (**1**) and *anti*-7-norbornenol (**2**) (Fig. 3), the only bond that can be rotated is the C–O bond. Thus **1** and **2** have only two conformers, which are defined by their C–O rotamers only. The rotamer where the OH bond in Newman projections of the C–O bond in secondary alcohols is located between two R-groups is denoted *Anti*. The other rotamer is denoted *Gauche*, in accordance with the denotations introduced in Ref. [62]. Thus the conformers of **1** and **2** are denoted *Anti* and *Gauche*, where *Gauche* has a multiplicity of 2 (Fig. 2). In the *Anti* conformation of **1** the O–H bond is situated almost directly above the C=C double bond and points towards it. This is the conformation which from visual inspection of models has a unique geometrical possibility for an intramolecular hydrogen bond.

4.1.1. IR and ^{1}H NMR spectroscopy

The IR data for *syn*-7-norbornenol (**1**) and *anti*-7-norbornenol (**2**) are given in Table 1. Literature data of **1** showed two bands at 3628 (18%) and 3575 cm^{-1} (82%) in the hydroxyl stretch region in IR, while literature data of **2** showed only one at 3632 cm^{-1}. Our data for **1** was close to the result from the most recent study [31] with the exception that we observed a band at 3590 cm^{-1}, caused by an unidentified impurity. When corrected for this spurious band, **1** has two bands at 3628 (20%) and 3575 cm^{-1} (80%), 53 cm^{-1} apart. This appears to be the first time the relative areas of the hydroxyl stretch bands have been reported as the result of a numerical analysis. The low frequency band is 21 cm^{-1} lower than that of 3-buten-1-ol (**5**, 3596 cm^{-1} [17]) and 14 cm^{-1} lower than that of epicholesterol (**7,** 3589 cm^{-1} [17]), which both were found to be intramolecularly hydrogen bonded. For comparison, the low frequency band of 3-cyclopenten-1-ol (**6**), which was found not to be intramolecularly hydrogen bonded, absorbed at 3601 cm^{-1} [17].

Consequently, band 2 (80%) of **1** is assigned to the *Anti* conformer with a significant O–H$\cdots\pi$ intramolecular hydrogen bond. Band 1 (20%) is then assigned to the *Gauche* conformer. The population of the hydrogen bonded conformer is, however, somewhat uncertain. It has been reported [3] that hydrogen bonding increases the hydroxyl stretch molecular absorption coefficient (band 2). However, this relationship is not always true in case of intramolecular hydrogen bonding [10]. Furthermore, it has also been reported that bands of Type II [62–65] (*Gauche*, band 1) might have a larger hydroxyl stretch molecular absorption coefficient than bands of Type III (*Anti*, band 2) due to differences in delocalisation possibilities [63]. This situation makes population estimates from IR rather uncertain.

The high frequency bands of both **1** (3628 cm^{-1}) and **2** (3632 cm^{-1}) absorbed at approximately the same frequencies close to the standard frequency for Type II rotamers (3627 cm^{-1} [62–65]). This indicates that **2** exists predominately in its *Gauche* conformer since **2** shows only one band.

^{1}H NMR spectroscopy gives important information on the conformational composition, especially the ^3J vicinal coupling constant. The observed coupling constants are the weighted average of the coupling constants for each of the three rotamers around each bond. For the H–C–O–H vicinal coupling constant, $J_{180°} = 12.5$ Hz has been proposed when the dihedral angle H–C–O–H = 180° and $J_{60°} = 2.2$ Hz when this dihedral angle equals 60° [12,13,66]. This gives

Table 3
Ab initio calculated hydroxyl group geometries for the conformers of *syn*-7-norbornenol (**1**) and *anti*-7-norbornenol (**2**). The values for the corresponding parameters for the *Gauche* and *Anti* conformers of the secondary alcohol 2-propanol is given in parenthesis. For notations, see Fig. 2. For simplicity, the same notation as for **1** is used for **2** in this table

Method	*Syn*-7-Norbornenol (2-propanol)			*Anti*-7-Norbornenol		
	Gauche	*Anti*	*Δ*	*Gauche*	*Anti*	*Δ*
O^8–H^H bond lengths (Å)						
HF/3-21G	0.9659 (0.9666)[a]	0.9668 (0.9675)[a]	+ 0.0009 (+0.0009)[a]	0.9662	0.9635	− 0.0027
HF/6-31G**	0.9427 (0.9430)[a]	0.9443 (0.9440)[a]	+ 0.0016 (+0.0010)[a]	0.9429	0.9418	− 0.0011
HF/6-31++G**	0.9428 (0.9430)[a]	0.9445 (0.9440)[a]	+ 0.0017 (+0.0010)[a]	0.9428	0.9421	− 0.0007
HF/6-31++G(2d,2p)	0.9396 (0.9398)	0.9415 (0.9409)	+ 0.0019 (+0.0011)	0.9397	0.9390	− 0.0007
MP2(FU)/6-31G**	0.9643 (0.9644)[a]	0.9675 (0.9655)[a]	+ 0.0032 (+0.0011)[a]	0.9648	0.9640	− 0.0008
MP2(FU)/6-31++G**	0.9660 (0.9661)	0.9694 (0.9672)	+ 0.0034 (+0.0011)	0.9661	0.9660	− 0.0001
C^7–O^8–H^H bond angles (°)						
HF/3-21G	110.93 (110.56)[a]	109.40 (109.77)[a]	− 1.53 (−0.79)[a]	110.97	111.93	+ 0.96
HF/6-31G**	109.70 (109.81)[a]	108.91 (109.51)[a]	− 0.79 (−0.31)[a]	109.70	111.37	+ 1.67
HF/6-31++G**	110.36 (110.55)[a]	109.83 (110.35)[a]	− 0.53 (−0.20)[a]	110.35	112.06	+ 1.71
HF/6-31++G(2d,2p)	110.03 (110.15)	109.45 (109.98)	− 0.58 (−0.17)	109.97	111.69	+ 1.72
MP2(FU)/6-31G**	107.24 (107.29)[a]	105.38 (106.58)[a]	− 1.86 (−0.71)[a]	107.29	108.14	+ 0.85
MP2(FU)/6-31++G**	108.27 (108.31)	106.77 (107.81)	− 1.50 (−0.50)	108.28	109.25	+ 0.97
H^C–C^7–O^8–H^H dihedral angles (°)						
HF/3-21G	73.3 (61.1)[a]	180.0		58.8	180.0	
HF/6-31G**	64.2 (59.6)[a]	180.0		56.8	180.0	
HF/6-31++G**	62.4 (60.5)[a]	180.0		51.8	180.0	
HF/6-31++G(2d,2p)	62.4 (61.0)	180.0		53.5	180.0	
MP2(FU)/6-31G**	64.4 (61.8)[a]	180.0		57.8	180.0	
MP2(FU)/6-31++G**	65.8 (65.2)	180.0		51.5	180.0	

[a] Ref. [62].

$J_{Anti} = 12.5$ Hz and $J_{Gauche} = 2.2$ Hz for secondary alcohols. Based on the observed $^3J_{CH-OH}$ (12.4 Hz) at high dilution in non-polar solution, *syn*-7-norbornenol (**1**) consists of 99% *Anti* and 1% *Gauche* conformers (Fig. 2).

In conclusion at this point, the IR and the ^{1}H NMR investigations indicated that between 80% (IR) and 99% (NMR) of compound **1** existed in the *Anti* conformation with a hydrogen bond to the π-electrons of the double bond. Due to the uncertainties in the

Table 4
Ab initio calculated hydroxyl stretch frequencies (cm^{-1}) and integrated intensities (in parenthesis, km mol^{-1}) for the conformers of *syn*-7-norbornenol (**1**) and *anti*-7-norbornenol (**2**). The frequencies are scaled. The scale factors are given in Table 8. HF/3-21G scale factor: 0.95163 [62]

Method	*Syn*-7-Norbornenol			*Anti*-7-Norbornenol		
	Gauche	*Anti*	*Δ*	*Gauche*	*Anti*	*Δ*
HF/3-21G	3681.0 (14)	3684.2 (17)	+ 3.2	3679.8 (18)	3728.4 (10)	+ 48.6
HF/6-31G**	3673.7 (46)	3656.3 (40)	− 17.4	3672.5 (53)	3694.1 (30)	+ 21.6
HF/6-31++G**	3673.1 (59)	3652.5 (47)	− 20.6	3674.5 (67)	3688.2 (36)	+ 13.7
HF/6-31++G(2d,2p)[a]	3673.4 (61)	3650.8 (46)	− 22.6	3673.2 (67)	3687.6 (36)	+ 14.4
MP2(FU)/6-31G**	3650.2 (24)	3606.4 (19)	− 43.8	3646.7 (30)	3661.2 (14)	+ 14.5

[a] The corresponding values for the *Gauche* and *Anti* conformers of 2-propanol was 3671.9 and 3655.7 cm^{-1} (scaled), respectively.

Table 5
Ab initio calculated distances (Å) between the proton donor (OH) and proton acceptor functions (C=C) for the *Anti* conformer of *syn*-7-norbornenol (**1**) and the corresponding distances for the *Anti* conformer of *anti*-7-norbornenol (**2**). For notations, see Fig. 2

Method	*Syn*-7-Norbornenol		*Anti*-7-Norbornenol	
	$O^{8}\cdots C^{2}$	$H^{H}\cdots C^{2}$	O···C	(O)H···C
HF/3-21G	2.94	2.58	2.90	2.55
HF/6-31G**	2.92	2.56	2.90	2.54
HF/6-31++G**	2.93	2.59	2.90	2.56
HF/6-31++G(2d,2p)	2.93	2.58	2.90	2.56
MP2(FU)/6-31G**	2.91	2.49	2.89	2.49
MP2(FU)/6-31++G**	2.93	2.53	2.91	2.52

estimates of the molecular absorption coefficients of the two IR bands of **1**, we suggest that **1** exists almost exclusively in the *Anti* form with an intramolecular hydrogen bond.

4.1.2. Theoretical calculations

Syn-7-Norbornenol (**1**) and *anti*-7-norbornenol (**2**) have previously only been subjects to a limited HF/STO-3G study by Morokuma et al. [36]. Only the *Anti* conformers and the maxima with O–H bonds pointing in the opposite directions were investigated by these workers.

Our results are tabulated in Tables 2–5, and the MP2/6-31++G** minimum energy structures are given in Fig. 3. In Table 2 we present the calculated populations of the two conformers *Anti* (multiplicity = 1) and *Gauche* (multiplicity = 2) of **1** and **2**. The results depend strongly on the method, demonstrating the need for high-level methods in describing the weak hydrogen bond interaction properly.

All molecular mechanics calculations on **1** severely underestimates the population of the *Anti* conformer (99% *Anti* from ^{1}H NMR). However, for **2**, the molecular mechanics populations are more in agreement with the presence of only one hydroxyl stretch band in IR at a frequency compatible with a Type II rotamer (*Gauche*) and with the results from the ab initio calculations. Using semiempirical MO theory, the *Anti* conformer of **1** was severely underestimated using MNDO. No *Gauche* minimum were found for **1** using AM1 and PM3 and no *Gauche* minimum was found for **2** using PM3. Using MNDO, the populations for **2** are more correctly described, while AM1 underestimates the population of the *Gauche* conformer.

The minimal HF/STO-3G calculations underestimates the *Anti* conformer of **1** (88%). However, all the other ab initio calculations, even the calculations with the small basis set 3-21G (HF), showed that *syn*-7-norbornenol (**1**) exists as 98–100% *Anti* as compared to 99% *Anti* from ^{1}H NMR. The energy differences between the *Gauche* and the *Anti* conformers were calculated to 3.8 kcal mol^{-1} (HF/3-21G), 2.6–2.8 kcal mol^{-1} (HF calculations with basis sets based on 6-31G) and 3.0–3.3 kcal mol^{-1} (MP2 calculations with basis sets based on 6-31G).

For *anti*-7-norbornenol (**2**), the ab initio calculations all showed that 90–96% of the molecules exists as *Gauche* conformers, in correspondence with the finding of only one hydroxyl stretch band in IR at a frequency compatible with a Type II rotamer. The energy differences between the *Gauche* and *Anti* conformers were calculated to 1.2–1.4 kcal mol^{-1} (HF) and 0.9–1.0 kcal mol^{-1} (MP2).

The calculated O–H bond lengths, C–O–H bond angles and H–C–O–H dihedral angles for the various ab initio calculations on the *Gauche* and *Anti* conformers of **1**, **2** and the secondary alcohol 2-propanol (reference) are tabulated in Table 3. The HF/3-21G calculations are obviously inadequate, and will not be further commented upon. The O–H bonds of *Anti* conformers of secondary alcohols are typically longer than in their corresponding *Gauche* conformers [62–65]. The calculated O–H bond lengths for the *Gauche* conformer of **1** are within ±0.0003 Å of the calculated bond lengths for the *Gauche* conformer of 2-propanol. The difference in O–H bond length between the *Anti* and *Gauche* conformers of **1** was calculated to 0.0016–0.0019 Å (HF) and 0.0032–0.0034 Å (MP2), compared to 0.0010–0.0011 Å (HF and

MP2) for the difference in O–H bond length between the *Anti* and *Gauche* conformers of 2-propanol. This shows that the O–H bond length in the *Anti* conformer of **1** is slightly, but significantly, prolonged due to intramolecular hydrogen bonding. The effect was much more substantial at the correlated level compared to the uncorrelated level, indicating the importance of electron correlation in hydrogen bonding. The ab initio calculations also showed that the C–O–H bond angles in **1** are decreased by 0.5–2° in the *Anti* conformer relative to the *Gauche* conformer, somewhat larger than the decrease for the corresponding conformers of 2-propanol (0.2–0.7°). This also indicates intramolecular hydrogen bonding.

For **2**, the calculated O–H bond lengths for the *Gauche* conformer was within ±0.0005 Å of the calculated bond lengths for the *Gauche* conformer of 2-propanol. However, in the *Anti* conformer, the O–H bond length was shortened (instead of prolonged as for 2-propanol) and the C–O–H bond angle increased compared to the *Gauche* conformer. The reason for this is most likely steric repulsion between the hydroxyl group and the upward pointing CH_2–CH_2 hydrogen atoms (Table 3).

We have also calculated the hydroxyl stretch frequencies for **1** and **2**. The results are tabulated in Table 4. All ab initio calculations in the table (except the calculations with the rudimentary basis set 3-21G) indicate that the *Anti* conformer of **1** should have a band at lower frequency than the *Gauche* band. The MP2 red shift of 44 cm^{-1} is in good agreement with the corresponding experimental number (CCl_4), which is 53 cm^{-1}. This is in line with our previous findings [17,62].

The fact that the O–H bond length of the *Anti* conformer of **2** is shorter than that of the *Gauche* conformer also influences the hydroxyl stretch frequency pattern. In contrast to **1**, the *Anti* conformer of **2** is calculated to be higher in frequency (15–22 cm^{-1}) than the *Gauche* conformer (ignoring the 3-21G calculations). We also note that the absolute value of the calculated frequency difference decreases upon increasing the basis set. This is opposite to the effect seen for **1**. For both **1** and **2**, the *Gauche* conformers are calculated to have approximately the same frequency. Consequently, the assignment of the IR bands to the conformers for **1** and **2** from IR only is still valid. No high frequency band for the *Anti* conformer of **2** was observed in high dilution IR spectroscopy (Table 1). We have previously reported such discrepancies from the standard frequency pattern [62–65] for Conformer **14** of 3-buten-1-ol (**5**) [17] and 2,2-dimethylpropanol [62].

The distances $O^8\cdots C^2$ and $H^H\cdots C^2$ for **1** and **2** are tabulated in Table 5. Irrespective of the quality of the wave function, the $O^8\cdots C^2$ and $H^H\cdots C^2$ distances of **1** are shorter than the sum of the van der Waals radii, confirming that **1** is intramolecularly hydrogen bonded [8,57,67,68]. For comparison, the calculated hydrogen bond distances are approximately 0.05–0.1 Å shorter than those to C^3 for Conformer **13** of 3-buten-1-ol (**5**) (HF/6-31G**) [17].

4.2. Methanol-ethene hydrogen bonded complex

In order to understand how intramolecular O–H$\cdots\pi$ hydrogen bonding influences the structural properties of *syn*-7-norbornenol (**1**) and other homoallylic alcohols, a more detailed and accurate quantum chemical study of a realistic model system would be useful. The methanol–ethene complex was considered to be ideal. A key feature of this complex is that the proton donor and acceptor functions are completely free to arrange themselves relative to each other. The water–ethene complex has been studied quite extensively, but we consider a system in which the O–H moiety is a part of an alcohol to be more relevant for the present purpose, because there is only one O–H bond to consider.

4.2.1. General considerations

Accurate calculations of the extremely fragile O–H$\cdots\pi$ bond requires certain methodological precautions. This has been discussed various places in the literature [57,69], but it is necessary to outline the most important facts here.

The basis set is of utmost importance. A poorly designed basis set or a too small basis set will lead to errors in the various factors that contribute to an hydrogen bond. The basis set superposition error (BSSE) is another complicating factor. Small basis sets tend to be subject to larger BSSE than larger basis sets. In addition to an artificial higher interaction energy, BSSE gives an artificial shortening of the hydrogen bond length.

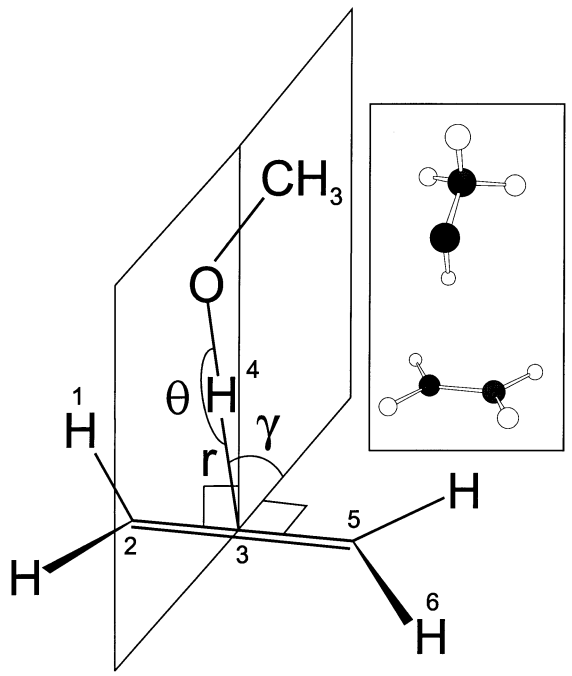

Fig. 4. Structural parameters of the methanol–ethene complex **8** (C_s). The methanol H–O–C plane is located perpendicular to and bisects the ethene C=C bond, r is the distance between the mid-point of the C=C double bond and the hydroxyl proton. γ defines the angle between the ethene plane and the line between the hydroxyl proton and the centre of the double bond. However, the ethene molecule is not planar in the complex and the reported value for γ is the dihedral angle 1-2-3-4 (the sum of the dihedral angles 1-2-3-4 and 6-5-3-4 was calculated to 180–181° (HF/MP2)). The angle θ defines the deviation from a straight line ($\theta = 180°$) between the centre of the double bond, the hydroxyl proton and the oxygen atom.

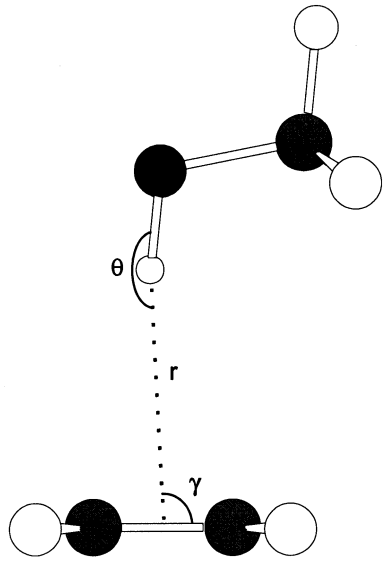

Fig. 5. Structural parameters of the ab initio transition structure or higher order saddle point for the methanol–ethene complex **9** (C_s). The methanol H–O–C plane is located perpendicular to the plane through the ethene hydrogen atoms and intersects the carbon atoms in the ethene C=C bond. r is the distance between the mid-point of the C=C double bond and the hydroxyl proton. γ defines the angle between the C=C bond and the line between the hydroxyl proton and the centre of the double bond. The angle θ defines the deviation from a straight line ($\theta = 180°$) between the centre of the double bond, the hydroxyl proton and the oxygen atom.

A Hartree–Fock wave function may in many respects be adequate, and provide reasonable estimates of the basic properties of an intermolecular hydrogen bond; the interaction energy, the equilibrium geometry and vibrational frequencies. Unfortunately, this success depends on cancellation between various sources of error. It turns out that electron correlation needs to be included to give a proper description of electrostatic and dispersion interactions. The contribution of the first may be either repulsive or attractive. The latter strengthens the hydrogen bond, giving an increased interaction energy, a shorter hydrogen bond length, a larger X–H (in this case O–H) bond length and a shorter frequency ν_{XH} (ν_{OH}) accompanied by a larger intensity I_{XH} (I_{OH}).

In the present work the MP2 method has been used to estimate electron correlation effects. Scheiner et al. have reported that the MP3 and MP4 contributions without BSSE correction to the total energy of several hydrogen bonded complexes are of approximately the same value, but with opposite signs, making MP2 a good approximation. With BSSE correction, the MP3 and MP4 contributions both approach zero when the basis set is increased [57]. Møller–Plesset calculations are size consistent [57] and among the computationally fast correlation methods and are thus easy to extend to larger basis sets [70].

The interaction energies were corrected for BSSE [56,57] using the full counterpoise (CP) method [58]. The CP method has been criticised for both overestimating and underestimating the true BSSE. Some researchers have defended the full counterpoise correction while others have proposed their own

Table 6
Interaction energy calculations for the methanol–ethene complex **8** (C_s). Total energies in hartrees, counterpoise corrections and interaction energies in kcal mol^{-1}

Method[a]	Number of basis functions	Number of imaginary frequencies	Total energies[b]			ΔE	Counterpoise			ΔE_{CP}[c]	ΔE_{CP} (MP2) $-\Delta E_{CP}$ (HF)
			Complex (C_s)	MeOH (C_s)	Ethene (D_{2h})		MeOH	Ethene	Total		
HF/6-31G**	100	0	− 193.08911	− 115.04671	− 78.03884	− 2.23	0.13	0.64	0.77	− 1.46	
HF/6-31++G**	124	0	− 193.09807	− 115.05251	− 78.04317	− 1.50	0.15	0.07	0.22	− 1.28	
HF/6-31++G(2d,2p)	172	0	− 193.10717	− 115.05841	− 78.04649	− 1.43	0.08	0.09	0.17	− 1.26	
HF/6-311++G**	144	0	− 193.13882	− 115.08051	− 78.05611	− 1.38	0.14	0.03	0.17	− 1.21	
HF/6-311++G(2d,2p)	188	0	− 193.14890	− 115.08565	− 78.06109	− 1.35	0.10	0.02	0.13	− 1.23	
HF/6-311++G(3df,3pd)//HF/6-311++G(2d,2p)	300	N/A	− 193.15609	− 115.09056	− 78.06330	− 1.40	0.08	0.11	0.18	− 1.21	
HF/cc-pVDZ	96	0	− 193.09266	− 115.04973	− 78.04017	− 1.73	0.24	0.31	0.55	− 1.18	
HF/cc-pVTZ	232	0	− 193.15698	− 115.09020	− 78.06442	− 1.48	0.21	0.10	0.31	− 1.18	
HF/cc-pVQZ	460	Not calculated[d]	− 193.17171	− 115.09983	− 78.06974	− 1.34	0.10	0.04	0.14	− 1.20	
HF/aug-cc-pVDZ	164	0	− 193.10817	− 115.06218	− 78.04371	− 1.43	0.05	0.16	0.21	− 1.22	
HF/aug-cc-pVTZ	368	0	− 193.16039	− 115.09309	− 78.06525	− 1.28	0.04	0.04	0.08	− 1.21	
HF/aug-cc-pVQZ	688	Not calculated[d]	− 193.17266	− 115.10070	− 78.07000	− 1.23	0.01	0.01	0.02	− 1.21	
MP2(FU)/6-31G**	100	0	− 193.72281	− 115.38984	− 78.32723	− 3.60	0.57	1.18	1.75	− 1.85	− 0.39
MP2(FU)/6-31++G**(#1)[e]	124	0	− 193.74105	− 115.40207	− 78.33367	− 3.34	0.53	0.97	1.50	− 1.83	− 0.55
MP2(FU)/6-31++G**(#2)[e]	124	0	− 193.74104	− 115.40207	− 78.33367	− 3.33	0.62	0.88	1.50	− 1.83	
MP2(FU)/6-31++G(2d,2p)	172	1	− 193.81294	− 115.44777	− 78.35915	− 3.78	0.49	0.92	1.41	− 2.37	− 1.11
MP2(FU)/6-311++G**	144	0	− 193.87224	− 115.48307	− 78.38395	− 3.27	0.53	0.73	1.26	− 2.00	− 0.79
MP2(FU)/6-311++G(2d,2p)	188	1	− 193.93140	− 115.51784	− 78.40828	− 3.31	0.42	0.38	0.79	− 2.52	− 1.29
MP2(FU)/6-311++G(3df,3pd)//MP2(FU)/6-311++G**	300	N/A	− 194.01735	− 115.56728	− 78.44428	− 3.63	0.36	0.53	0.89	− 2.74	
MP2(FU)/cc-pVDZ	96	0	− 193.71864	− 115.39292	− 78.32029	− 3.41	1.03	0.84	1.86	− 1.55	
MP2(FU)/cc-pVTZ	232	0	− 193.98269	− 115.54686	− 78.43000	− 3.66	0.79	0.43	1.22	− 2.44	
MP2(FU)/cc-pVQZ//MP2(FU)/cc-pVTZ	460	N/A	− 194.10346	− 115.61691	− 78.48120	− 3.36	0.34	0.22	0.56	− 2.80	
MP2(FU)/aug-cc-pVDZ	164	Not calculated[d]	− 193.76834	− 115.42756	− 78.33442	− 3.99	0.50	0.98	1.48	− 2.51	
MP2(FU)/aug-cc-pVTZ	368	Not calculated[d]	− 194.00925	− 115.56263	− 78.43998	− 4.17	0.58	0.74	1.32	− 2.85	
MP2(FU)/aug-cc-pVTZ//MP2(FU)/cc-pVTZ	368	N/A	− 194.00920	− 115.56258	− 78.43997	− 4.17	0.57	0.73	1.30	− 2.88	
MP2(FC)/cc-pVDZ	96	0	− 193.70866	− 115.38797	− 78.31530	− 3.38	1.01	0.81	1.82	− 1.56	− 0.38
MP2(FC)/cc-pVTZ	232	Not calculated[d]	− 193.92234	− 115.51748	− 78.39931	− 3.49	0.67	0.36	1.02	− 2.47	− 1.29

Table 6 (*continued*)

Method[a]	Number of basis functions	Number of imaginary frequencies	Total energies[b]			ΔE	Counterpoise			ΔE_{CP}[c]	ΔE_{CP} (MP2) $-\Delta E_{CP}$ (HF)
			Complex (C_s)	MeOH (C_s)	Ethene (D_{2h})		MeOH	Ethene	Total		
MP2(FC)/cc-pVQZ// MP2(FC)/cc-pVTZ	460	N/A	− 193.98880	− 115.55829	− 78.42527	− 3.29	0.31	0.16	0.48	− 2.81	− 1.61
MP2(FC)/aug-cc-pVDZ	164	Not calculated[d]	− 193.75692	− 115.42193	− 78.32892	− 3.81	0.44	0.84	1.28	− 2.53	− 1.31
MP2(FC)/aug-cc-pVTZ// MP2(FU)/aug-cc-pVTZ	368	N/A	− 193.93904	− 115.52898	− 78.40447	− 3.51	0.27	0.37	0.65	− 2.86	− 1.65
MP2(FC)/aug-cc-pVQZ// MP2(FU)/aug-cc-pVTZ	688	N/A	− 193.99593	− 115.56311	− 78.42767	− 3.23	0.11	0.16	0.27	− 2.96	− 1.75

[a] Fully optimised at the indicated level.
[b] Vibrational zero point energy not included.
[c] Counterpoise corrected.
[d] Optimised without second analytical derivatives.
[e] Two minima.

Table 7
Ab initio calculated geometry parameters for the methanol–ethene complex **8** (C_s) as compared with methanol (C_s)s. For notations, see Fig. 4

Method	γ (°)	θ (°)	r (Å)	O···C (Å)	(O)H···C (Å)	O–H (Å)			C–O–H (°)		
						MeOH	**8**	Δ	MeOH	**8**	Δ
HF/6-31G**	96.66	182.06	2.68	3.68	2.76	0.9423	0.9437	0.0014	109.64	109.50	− 0.14
HF/6-31++G**	101.92	175.15	2.77	3.77	2.85	0.9423	0.9436	0.0013	110.55	110.41	− 0.14
HF/6-31++G(2d,2p)	101.71	174.03	2.77	3.76	2.84	0.9391	0.9407	0.0016	110.03	109.95	− 0.08
HF/6-311++G**	100.21	177.82	2.81	3.81	2.88	0.9397	0.9410	0.0013	110.01	109.87	− 0.14
HF/6-311++G(2d,2p)	100.53	175.61	2.78	3.78	2.86	0.9381	0.9395	0.0014	110.10	110.00	− 0.10
HF/cc-pVDZ	97.64	183.69	2.72	3.72	2.80	0.9449	0.9460	0.0011	109.09	108.94	− 0.16
HF/cc-pVTZ	99.46	178.60	2.75	3.75	2.83	0.9390	0.9403	0.0013	109.92	109.84	− 0.08
HF/cc-pVQZ	99.50	178.48	2.78	3.78	2.86	0.9380	0.9392	0.0012	110.23	110.10	− 0.13
HF/aug-cc-pVDZ	99.18	176.84	2.77	3.77	2.84	0.9420	0.9434	0.0014	109.98	109.86	− 0.12
HF/aug-cc-pVTZ	101.36	173.98	2.78	3.77	2.86	0.9393	0.9406	0.0013	110.25	110.18	− 0.08
HF/aug-cc-pVQZ	101.40	173.99	2.80	3.79	2.87	0.9381	0.9394	0.0013	110.22	110.21	− 0.01
MP2(FU)/6-31G**	94.56	189.08	2.39	3.41	2.48	0.9622	0.9640	0.0018	107.33	106.73	− 0.60
MP2(FU)/6-31++G**(#1)	113.37	165.73	2.38	3.39	2.47	0.9637	0.9657	0.0020	108.57	108.36	− 0.21
MP2(FU)/6-31++G**(#2)	85.40	195.71	2.43	3.43	2.52	0.9637	0.9661	0.0024	108.57	107.79	− 0.78
MP2(FU)/6-31++G(2d,2p)	92.46	185.16	2.32	3.35	2.41	0.9592	0.9629	0.0037	108.01	107.35	− 0.66
MP2(FU)/6-311++G**	90.54	195.55	2.43	3.44	2.53	0.9589	0.9612	0.0023	107.40	106.58	− 0.82
MP2(FU)/6-311++G(2d,2p)	92.70	189.57	2.36	3.38	2.45	0.9570	0.9604	0.0034	108.13	107.36	− 0.77
MP2(FU)/cc-pVDZ	89.22	194.64	2.36	3.37	2.46	0.9652	0.9665	0.0013	106.29	105.71	− 0.58
MP2(FU)/cc-pVTZ	91.72	190.63	2.32	3.33	2.41	0.9581	0.9610	0.0029	107.56	106.88	− 0.68
MP2(FU)/aug-cc-pVDZ	91.57	190.87	2.34	3.37	2.44	0.9657	0.9685	0.0028	107.92	106.91	− 1.00
MP2(FU)/aug-cc-pVTZ	91.16	191.07	2.30	3.32	2.40	0.9590	0.9615	0.0025	108.14	107.12	− 1.01
MP2(FC)/cc-pVDZ	89.22	194.70	2.37	3.38	2.46	0.9655	0.9670	0.0015	106.33	105.69	− 0.65
MP2(FC)/cc-pVTZ	91.74	190.56	2.34	3.35	2.43	0.9594	0.9626	0.0032	107.43	106.79	− 0.64
MP2(FC)/aug-cc-pVDZ	91.39	191.16	2.36	3.38	2.46	0.9657	0.9690	0.0033	107.94	106.92	− 1.02

variant [57,71–77]. Nevertheless, there seems to be a consensus that the CP correction gives a correct order-of-magnitude estimate of BSSE [78].

When high accuracy is aimed for, it is insufficient to carry out single calculations. A more systematic approach is needed, like e.g. the Dunning's correlation consistent basis sets which offer a systematic improvement to the correlation energy with each increment in the cardinal number [53–55,78]. It has been found that the correlation energies obtained with these basis sets converge smoothly to apparent complete basis set limits [78,79] as demonstrated by Feller [70,80]. Many other properties also converge to well-defined limits [79].

4.2.2. Results

We performed ab initio molecular orbital calculations on the two methanol–ethene complexes with C_s symmetry, **8** and **9**, as defined in Figs. 4 and 5. The results from the calculations on **8** are shown in Tables 6–8. The geometry optimisations and frequency calculations on **9** were done with various basis sets up to 6-311++G(2d,2p), using both HF and MP2. The calculations revealed that the potential energy surface (PES) is very flat with respect to variations of θ and γ (Fig. 6; see Fig. 4 for definitions). In most cases **8** was found to be a minimum (with zero imaginary frequencies), while **9** was found to be a transition structure or a higher order saddle point. The energy differences were less than 0.3 kcal mol^{-1}. Furthermore, the absolute value of the imaginary frequency in the two cases where **8** was found to be a transition structure was below 20 cm^{-1}, which probably is of the order of the numerical precision. The substantial decrease in the distance r in going from HF to MP2 (Table 7 and Fig. 7) results from not including the attractive dispersion forces in the former wave function.

The calculated HF and MP2 interaction energies for **8** are summarised in Table 6. With HF, all the calculations gave uncorrected interaction energies in the range −1.2–1.5 kcal mol^{-1} with the exception of

Table 8
Ab initio calculated hydroxyl stretch frequencies[a] (ν, cm^{-1}), scale factors, frequency shifts[b] and integrated intensities (I, km mol^{-1}) for methanol (C_s) and the methanol–ethene complex **8** (C_s)

Method	ν_{OH} MeOH (C_s) (not scaled)	Scale factor[a]	ν_{OH} **8** (C_s) (scaled)	$\Delta\nu$[b] (scaled)	I_{OH} MeOH	I_{OH} **8**	I_{OH} (**8**)/I_{OH} (MeOH)
HF/6-31G**	4192.8	0.87794	3662.6	− 18.4	42	162	3.8
HF/6-31++G**	4197.1	0.87703	3662.7	− 18.3	55	168	3.1
HF/6-31++G(2d,2p)	4200.5	0.87632	3658.7	− 22.3	56	177	3.1
HF/6-311++G**	4190.2	0.87849	3664.3	− 16.7	57	162	2.8
HF/6-311++G(2d,2p)	4198.1	0.87682	3660.2	− 20.8	58	175	3.0
HF/cc-pVDZ	4155.3	0.88585	3668.0	− 13.0	53	164	3.1
HF/cc-pVTZ	4177.1	0.88124	3662.3	− 18.7	52	164	3.2
HF/aug-cc-pVDZ	4181.1	0.88038	3659.1	− 21.9	54	172	3.2
HF/aug-cc-pVTZ	4171.7	0.88237	3660.5	− 20.5	56	173	3.1
MP2(FU)/6-31G**	3915.0	0.94023	3653.6	− 27.4	22	179	8.3
MP2(FU)/6-31++G**(#1)	3899.6	0.94394	3646.5	− 34.5	32	225	7.0
MP2(FU)/6-31++G**(#2)	3899.6	0.94394	3641.6	− 39.4	32	188	5.8
MP2(FU)/6-31++G(2d,2p)	3887.2	0.94696	3606.5	− 74.5	37	280	7.6
MP2(FU)/6-311++G**	3918.1	0.93947	3640.2	− 40.8	36	189	5.2
MP2(FU)/6-311++G(2d,2p)	3903.3	0.94304	3618.8	− 62.2	40	251	6.2
MP2(FU)/cc-pVDZ	3869.3	0.95134	3659.3	− 21.7	29	194	6.6
MP2(FU)/cc-pVTZ	3896.7	0.94464	3628.9	− 52.1	36	248	6.8
MP2(FC)/cc-pVDZ	3868.7	0.95149	3656.7	− 24.3	29	192	6.6

[a] The frequencies are scaled based on the experimental (gas phase) and calculated values for OH stretch in methanol (experimental: 3681 cm^{-1} [81]).
[b] Calculated frequency shift (scaled frequencies) for the complex relative to the hydroxyl stretch frequency of methanol (3681 cm^{-1} [81]).

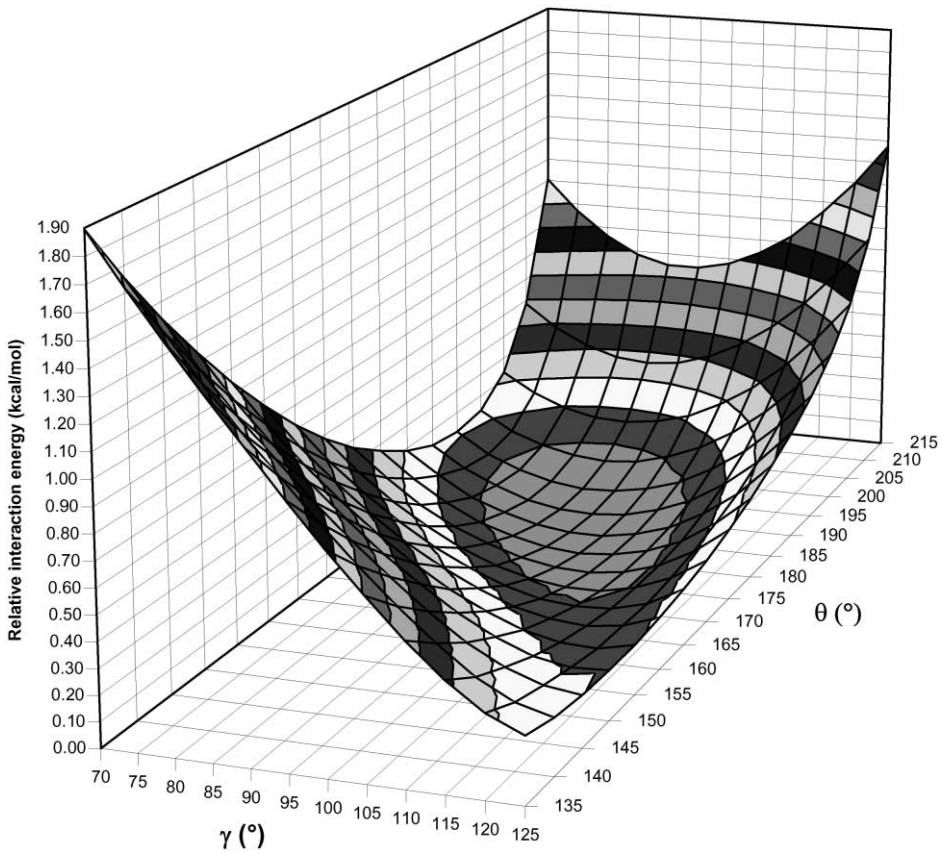

Fig. 6. Relative interaction energy for the methanol–ethene complex **8** (C_s) obtained using single point calculations (MP2(FU)/6-31G**) as a function of both θ and γ, starting with the fully optimised minimum energy structure at the same level of theory and keeping all other parameters constant. No correction for BSSE. For notations, see Fig. 4.

the two smallest basis sets, which gave somewhat higher absolute values due to BSSE. We observed that the counterpoise (CP) correction with HF was < 0.3 kcal mol^{-1} with the exception of the two smallest basis sets and that the CP corrected interaction energies all were in the range -1.2–1.3 kcal mol^{-1} with the exception of the 6-31G** calculations. This shows that, when using 6-31++G** or cc-pVTZ and larger basis sets, the HF interaction energies are not largely basis set dependent and that these basis sets are almost free of BSSE. The very large basis set aug-cc-pVQZ gave the smallest HF value for BSSE, 0.02 kcal mol^{-1}. The convergence of the interaction energy is shown in Fig. 8, using the method of Feller [70,80]. Extrapolation gives a HF interaction energy of approximately -1.2 kcal mol^{-1}, vibrational zero point energy not included.

The BSSE was greatly reduced with HF using fairly large basis sets. However, the BSSE is much less susceptible to reduction at correlated levels and is often non-negligible [57]. It is necessary to use a large flexible basis set with multiple polarisation and diffuse functions to accurately evaluate the interactions [18,70,75,78,80].

Our MP2 calculations were first done with the core electrons included (FU). However, Feller et al. [80] have recently pointed out that the Dunning's correlation consistent basis sets cc-pVxZ and aug-cc-pVxZ only were designed to recover valence correlation.

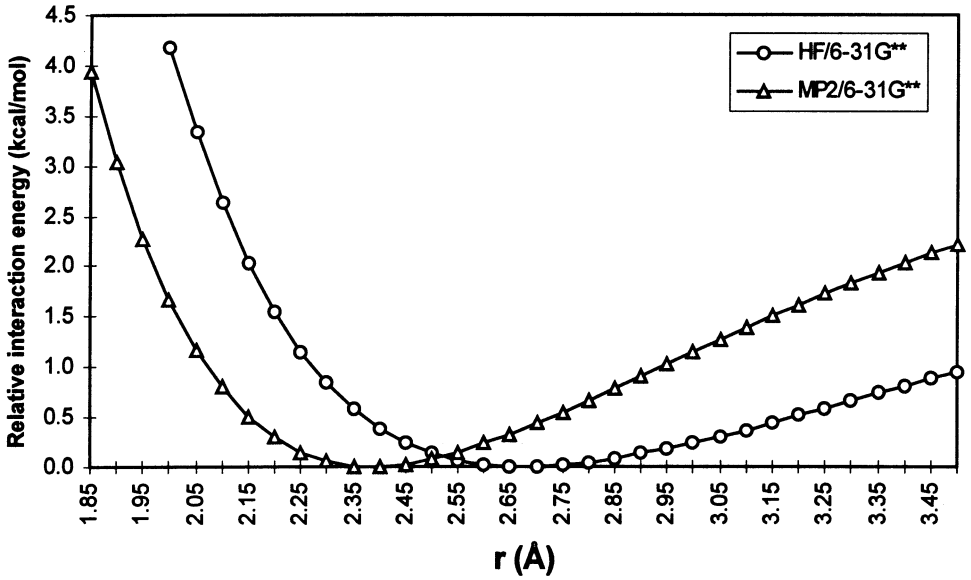

Fig. 7. Relative interaction energy for the methanol–ethene complex **8** (C_s) obtained using single point calculations (HF/6-31G** and MP2(FU)/6-31G**) as a function of r, starting with the fully optimised minimum energy structures at the same levels of theory and keeping all other parameters constant. No correction for BSSE. For notations, see Fig. 4.

Thus we also performed MP2 calculations using frozen core (FC). The geometries with and without core electrons in the MP2 calculations were found to be almost identical (Table 7). However, from Table 6 it is evident that the use of frozen core decreased the uncorrected absolute interaction energy and the BSSE, especially with aug-cc-pVxZ, while the CP corrected interaction energies are almost identical in both cases.

Due to the very flat PES around the minimum energy structure, some of the frozen core MP2 energy calculations were done using the corresponding MP2(FU) geometries. For the same reasons, some of the energy calculations were done on optimised geometries with smaller basis sets (Table 6). The effects of ignoring or including geometry relaxation is small as demonstrated by the MP2(FU)/aug-cc-pVTZ energy calculations with both relaxed and fixed geometry in Table 6.

As expected, the MP2 BSSE was quite large. It was reduced by approximately a factor of two when the cardinal number was increased by 1 [78] (Table 6). This was not the case for the MP2(FU)/aug-cc-pVxZ series where BSSE was hardly reduced by increasing the cardinal number. As expected [80], this was corrected by FC calculations. The smallest basis sets gave a BSSE of 1.9 kcal mol^{-1}. However, the very large basis set aug-cc-pVQZ reduced BSSE to 0.27 kcal mol^{-1}. We note that as the BSSE was gradually reduced by increasing the size of the basis set, the CP corrected absolute interaction energy was gradually increased while the uncorrected absolute interaction energy was gradually reduced [70,80] (Table 6, Fig. 9). When using the counterpoise procedure it is only possible to compensate partly for the missing part of the correlation energy for basis sets smaller than aug-cc-pVTZ. In this case it is necessary to use very large basis sets up to aug-cc-pVQZ to estimate the interaction energy of **8**. Extrapolation using the method of Feller [70,80] in Fig. 9 gives an interaction energy of approximately -3.1 ± 0.1 kcal mol^{-1}, vibrational zero point energy not included.

The large and almost systematic increase in the absolute difference between the CP corrected interaction energies for the uncorrelated (HF) and correlated (MP2) calculations with the same basis set upon increasing the number of basis functions shows that electron correlation is a very significant and non-negligible contribution to the interaction energy (Table 6, Figs. 8–9).

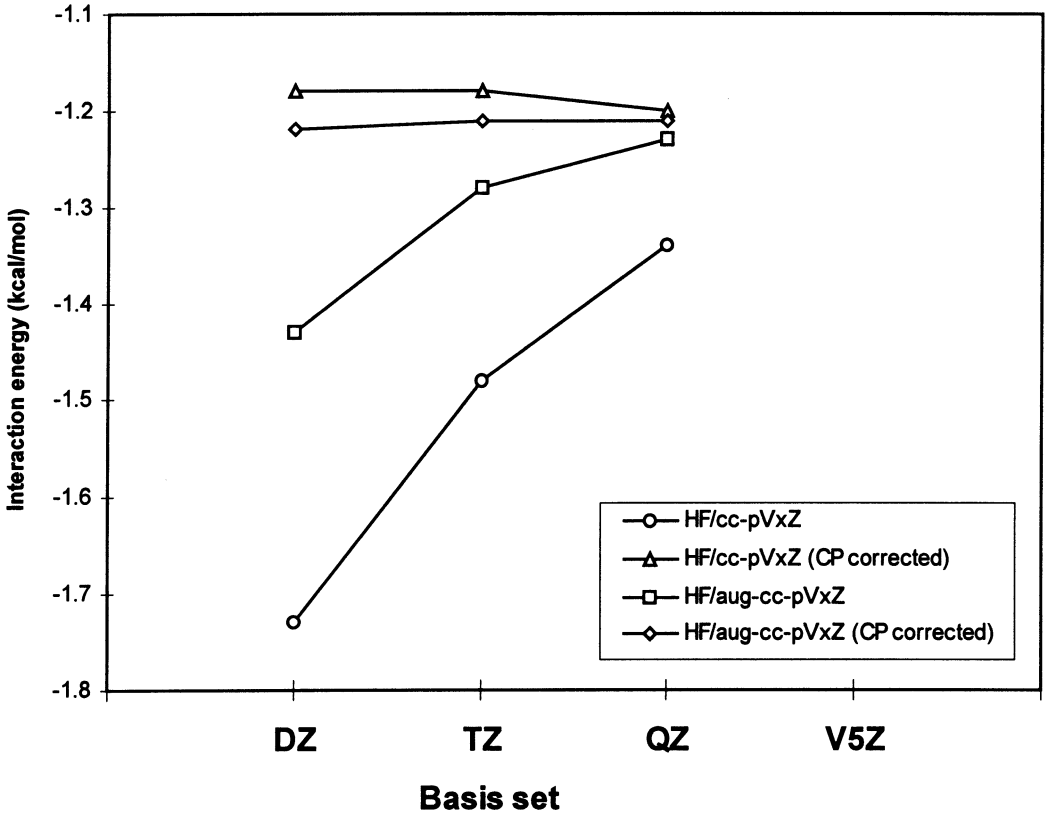

Fig. 8. Convergence of the HF interaction energies of **8** as a function of the size of the basis set using Dunning's correlation consistent basis sets cc-pVxZ and aug-cc-pVxZ (x = D through Q), with and without the counterpoise correction.

The HF calculations give a minimum energy structure with $\gamma = 99 - 102°$, $\theta = 174 - 179°$, $r = 2.75 - 2.81$ Å while the MP2 calculations give a minimum energy structure with $\gamma = 91 - 92°$, $\theta = 191 - 196°$, $r = 2.30 - 2.43$ Å (Table 7, the smallest basis sets and the calculations with imaginary frequencies and double minima were excluded). This shows that even if a very large basis set with MP2 is necessary to evaluate the interaction energy, the geometry of the complex is not so dependent upon the basis set used. The calculations with the largest basis sets gave $\gamma = 101°$, $\theta = 174°$, $r = 2.80$ Å (HF) and $\gamma = 91°$, $\theta = 191°$, $r = 2.30$ Å (MP2). With MP2 using Dunning's correlation consistent basis sets we observed that r decreased upon increasing the cardinal number. However, we may not have reached the asymptotic limit for r with MP2(FU)/aug-cc-pVTZ.

With MP2, the (O)H···C distances were, for all basis sets used, less than the sum of the van der Waals radii, confirming the hydrogen bonded nature of the interaction (see Table 7). The MP2 calculations with the largest basis set gave a distance of 2.40 Å, which is significantly less than the sum of the van der Waals radii (see also Section 4.1.2).

The differences in O–H bond length between methanol and **8** are also given in Table 7. The MP2 value of the O–H bond length increases by approximately 0.003 Å, and the MP2 C–O–H bond angle decreases by approximately 1.0°.

We also calculated the hydroxyl stretch frequencies for methanol and the methanol–ethene C_s complex (**8**). The result is shown in Table 8. With the largest basis set and MP2, the red shift for the complex is 52 cm^{-1}. The corresponding calculated integrated intensities for the complex is seven times that of methanol alone. The larger red shift and larger

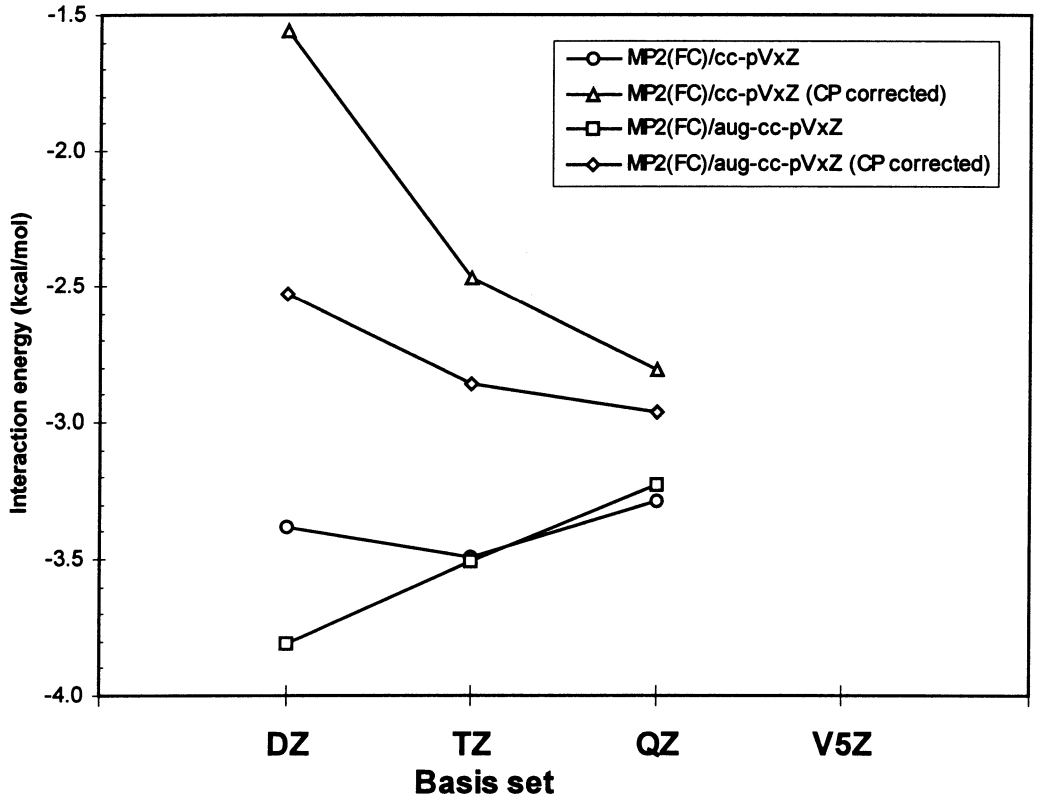

Fig. 9. Convergence of the MP2(FC) interaction energies of **8** as a function of the size of the basis set using Dunning's correlation consistent basis sets cc-pVxZ and aug-cc-pVxZ (x = D through Q), with and without the counterpoise correction.

intensity with MP2 compared to HF shows again the importance of electron correlation for intermolecular hydrogen bonding.

4.3. Comparisons between intra- and intermolecular hydrogen bonding

The calculations on both **1** and **8** showed prolongation of the O–H bond, a smaller C–O–H bond angle and a red frequency shift upon interaction. The effects are more substantial at the electron correlated level than with HF. The O···C and (O)H···C distances for **1** are all shorter than the sum of the van der Waals radii. The same is not the case for the complex **8** where only the MP2 (O)H···C distances are less then the sum of the van der Waals radii.

From Fig. 3 and Table 7 it is evident that the geometries of **1** and **8** are very different. The corresponding values to γ and θ (91 and 191°, respectively) in **8** (MP2/aug-cc-pVTZ) were for the *Anti* conformer of **1** ≈ 70 and 304.2°, respectively (MP2/6-31++G**).

The reason for this large difference in geometry is that in **1** the proton donor and acceptor functions are forced together by the strained skeleton while the calculations of **8** gives the minimum energy structure when the proton donor and acceptor functions can approach each other freely. However, an arrangement of the proton donor and acceptor functions as for **1** is not possible for the complex **8** due to steric conflicts between some of the ethene and methanol protons.

This makes the water–ethene complex without such conflicts an attractive probe for further investigations. This has, however, recently been investigated [24]. It was found to have a geometry (MP2/6-31++G(2d,2p) very similar to **8** with $r = 2.36$ Å, $\gamma = 71.46°$ and $\theta = 189.70°$. The interaction energy was estimated to -2.5 kcal mol^{-1} (MP2/NHFL(3d,2p)) in contrast to

-3.1 ± 0.1 kcal mol^{-1} for **8**. For comparison, the interaction in the water dimer has been estimated to -5.0 ± 0.1 kcal mol^{-1} [70,80] while the interaction energy for the methanol–water complex has been estimated to -4.9 kcal mol^{-1} [18]. These values are not corrected for vibrational zero point energy.

5. Conclusions

From IR, ^{1}H NMR and ab initio calculations, *syn*-7-norbornenol (**1**) was found to be intramolecularly hydrogen bonded and exist almost exclusively in its hydrogen bonded form, the *Anti* conformer (Fig. 3). The model compound *anti*-7-norbornenol (**2**), with no possibility for intramolecular hydrogen bonding, was found to exist as the *Gauche* conformer (Fig. 3). For **1**, many effects became more visible with the use of electron correlation.

The methanol–ethene intermolecularly hydrogen bonded complex was found to adopt two different, but similar, arrangements depending on the method of calculation (HF or MP2), both very different from the arrangement of the donor and acceptor functions in **1**. The PESes around the minimum energy structures are rather flat, with an almost freely rotating methanol part. At the correlated level it was necessary to use very large basis sets to reduce BSSE to estimate the interaction energy, while BSSE was small for all but the smallest basis sets with HF. Electron correlation was found to be a necessity since the attractive energies and the hydrogen bond distance were calculated to be artificially small with HF due to lack of dispersion. The MP2 interaction energies greatly depend on the basis sets while the HF and MP2 geometries and HF energies do not. The complete basis set limit for the HF interaction energy of the complex is estimated to -1.2 kcal mol^{-1} with an accompanying correlation contribution of -1.9 kcal mol^{-1}, which gives an interaction energy of -3.1 ± 0.1 kcal mol^{-1}, vibrational zero point energy not included. MP2/aug-cc-pVTZ calculations gave a geometry with $\gamma = 91°$, $\theta = 191°$, $r = 2.30$ Å (see Fig. 4 for definitions of the geometrical parameters).

Acknowledgements

Financial support for this research from The Norwegian Research Council for Science and the Humanities (NAVF) is gratefully acknowledged. This work has also received support from The Research Council of Norway (Programme for Supercomputing) through a grant of computing time (Cray X-MP/216, Cray Y-MP4D/464, Cray J916/8128 and Cray T3E in Trondheim).

References

[1] Latimer and Rodebush, J. Am. Chem. Soc. 42 (1920) 1419.
[2] L. Pauling, The Nature of the Chemical Bond, 3rd edn., Cornell University Press, New York, 1960, pp. 449–504.
[3] G.C. Pimentel, A.L. McClellan, The Hydrogen Bond, Freeman, San Francisco, 1960.
[4] D.A. Smith, in: D.A. Smith (Ed.), Modeling the Hydrogen Bond, ACS Symposium Series 569, American Chemical Society, Washington, DC, 1994 (Chapter 1).
[5] M.J. Calhorda, Chem. Commun. (2000) 801.
[6] H.S. Aaron, Top. Stereochem. 11 (1979) 1.
[7] M. Tichy, Adv. Org. Chem. 5 (1965) 115.
[8] F. Hibbert, J. Emsley, Adv. Phys. Org. Chem. 26 (1990) 255.
[9] P. Schuster, G. Zundel, C. Sandorfy (Eds.), The Hydrogen Bond. Recent Developments in Theory and Experiments, North Holland, Amsterdam, 1976.
[10] T. Dziembowska, Polish J. Chem. 68 (1994) 1455.
[11] R.J. Abraham, J.M. Bakke, Acta Chem. Scand., Ser. B 37 (1983) 865.
[12] J.M. Bakke, A.M. Schie, T. Skjetne, Acta Chem. Scand., Ser. B 40 (1986) 703.
[13] J.M. Bakke, D.J. Chadwick, Acta Chem. Scand., Ser. B 42 (1988) 223.
[14] J.M. Bakke, J. Krane, T. Skjetne, Acta Chem. Scand., Ser. B 43 (1989) 777.
[15] J.M. Bakke, L.H. Bjerkeseth, T.E.C.L. Rønnow, K. Steinsvoll, J. Mol. Struct. 321 (1994) 205.
[16] L.H. Bjerkeseth, Conformational Analysis of Alcohols with Weak Hydrogen Bonds (in Norwegian), Thesis, Norwegian Institute of Technology, Department of Organic Chemistry, Trondheim, Norway, 1994.
[17] J.M. Bakke, L.H. Bjerkeseth, J. Mol. Struct. 470 (1998) 247.
[18] S. Tsuzuki, T. Uchimaru, K. Matsumura, M. Mikami, K. Tanabe, J. Chem. Phys. 110 (1999) 11,906.
[19] J.E. Del Bene, Chem. Phys. Lett. 24 (1974) 203.
[20] A. Engdahl, B. Nelander, Chem. Phys. Lett. 113 (1985) 49.
[21] K.I. Peterson, W. Klemperer, J. Chem. Phys. 85 (1986) 725.
[22] A. Engdahl, B. Nelander, J. Phys. Chem. 90 (1986) 4982.
[23] B. Nelander, J. Phys. Chem. 92 (1988) 5642.
[24] M.C. Rovira, J.J. Novoa, M.-H. Whangbo, J.M. Williams, Chem. Phys. 200 (1995) 319.
[25] A.M. Andrews, R.L. Kuczkowski, J. Chem. Phys. 98 (1993) 791.

[26] J.H. Lii, N.L. Allinger, J. Phys. Org. Chem. 7 (1994) 591.
[27] R.K. Bly, R.S. Bly, J. Org. Chem. 28 (1963) 3165.
[28] L. Joris, P.v.R. Schleyer, R. Gleiter, J. Am. Chem. Soc. 90 (1968) 327.
[29] L.P. Kuhn, R.E. Bowman, R.S. Bly, R.K. Bly, L. Joris, P.v.R. Schleyer. To be published. Reference from Joris et al. [28].
[30] R.S. Brown, Can. J. Chem. 54 (1976) 3206.
[31] M. Takasuka, H. Tanida, J. Chem. Soc., Perkin Trans. II (1980) 486.
[32] E. Kantolahti, K. Laihia, Finn. Chem. Lett. (1975) 6.
[33] R.J. Ouellette, K. Liptak, G.E. Booth, J. Org. Chem. 32 (1967) 2394.
[34] K. Pihlaja, J. Jalonen, D.M. Jordan, Adv. Mass Spectrom. 6 (1974) 105.
[35] A. Gamba, P. Beltrame, M. Simonetta, Gaz. Chim. Ital. 101 (1971) 57.
[36] K. Morokuma, G. Wipff, Chem. Phys. Lett. 74 (1980) 400.
[37] W.C. Baird Jr., J. Org. Chem. 31 (1966) 2411.
[38] R.R. Sauers, R.M. Hawthorne Jr., J. Org. Chem. 29 (1964) 1685.
[39] E.I. Snyder, B. Franzus, J. Am. Chem. Soc. 86 (1964) 1166.
[40] T. Goto, A. Tatematsu, Y. Hata, R. Muneyuki, H. Tanida, K. Tori, Tetrahedron 22 (1966) 2213.
[41] J.B. Stothers, C.T. Tan, Can. J. Chem. 55 (1977) 841.
[42] N.L. Allinger, H.L. Flanagan, J. Comput. Chem. 4 (1983) 339 (as adapted by Serena Software, Bloomington, Indiana, USA).
[43] R.J. Abraham, G.H. Grant, B. Hudson, P.H. Smith, CHARGE2, University of Liverpool, UK. Modified by D.J. Chadwick for input of modified MNDO files.
[44] R.J. Abraham, L. Griffiths, P. Loftus, J. Comput. Chem. 3 (1982) 407.
[45] R.J. Abraham, B. Hudson, J. Comput. Chem. 5 (1984) 562.
[46] R.J. Abraham, B. Hudson, J. Comput. Chem. 6 (1985) 173.
[47] R.J. Abraham, P.E. Smith, J. Comput. Chem. 9 (1987) 288.
[48] J.J.P. Stewart, MOPAC ver. 6.00, Frank J. Seiler Research Laboratory, United States Air Force Academy, Colorado, USA, 1990.
[49] M.J. Frisch, M. Head-Gordon, G.W. Trucks, J.B. Foresman, H.B. Schlegel, K. Raghavachari, M.A. Robb, J.S. Binkley, C. Gonzalez, D.J. Defrees, D.J. Fox, R.A. Whiteside, R. Seeger, C.F. Melius, J. Baker, R.L. Martin, L.R. Kahn, J.J.P. Stewart, S. Topiol, J.A. Pople, GAUSSIAN 90, Revision I, Gaussian, Inc., Pittsburgh, Pennsylvania, USA, 1990.
[50] M.J. Frisch, G.W. Trucks, M. Head-Gordon, P.M.W. Gill, M.W. Wong, J.B. Foresman, B.G. Johnson, H.B. Schlegel, M.A. Robb, E.S. Reploge, R. Gomperts, J.L. Andres, K. Raghavachari, J.S. Binkley, C. Gonzalez, R.L. Martin, D.J. Fox, D.J. Defrees, J. Baker, J.J.P. Stewart, J.A. Pople, GAUSSIAN 92, Revision C and G.2, Gaussian, Inc., Pittsburgh, Pennsylvania, USA, 1992.
[51] M.J. Frisch, G.W. Trucks, H.B. Schlegel, P.M.W. Gill, B.G. Johnson, M.A. Robb, J.R. Cheeseman, T. Keith, G.A. Petersson, J.A. Montgomery, K. Raghavachari, M.A. Al-Laham, V.G. Zakrzewski, J.V. Ortiz, J.B. Foresman, J. Cioslowski, B.B. Stefanov, A. Nanayakkara, M. Challacombe, C.Y. Peng, P.Y. Ayala, W. Chen, M.W. Wong, J.L. Andres, E.S. Replogle, R. Gomperts, R.L. Martin, D.J. Fox, J.S. Binkley, D.J. Defrees, J. Baker, J.P. Stewart, M. Head-Gordon, C. Gonzalez, J.A. Pople, GAUSSIAN 94, Revision B.1 and D.4, Gaussian, Inc., Pittsburgh, Pennsylvania, USA, 1995.
[52] C. Møller, M.S. Plesset, Phys. Rev. 46 (1934) 618.
[53] T.H. Dunning Jr., J. Chem. Phys. 90 (1989) 1007.
[54] R.A. Kendall, T.H. Dunning Jr., R.J. Harrison, J. Chem. Phys. 96 (1992) 6796.
[55] D.E. Woon, T.H. Dunning Jr., J. Chem. Phys. 98 (1993) 1358.
[56] G.A. Yeo, T.A. Ford, J. Mol. Struct. (Theochem) 168 (1988) 247.
[57] S. Scheiner, in: K.B. Lipkowitz, D.B. Boyd (Eds.), Reviews in Computational Chemistry II, VCH Publishers, New York, 1991 (Chapter 5).
[58] S.F. Boys, F. Bernardi, Mol. Phys. 19 (1970) 553.
[59] M.J. Frisch, J.E. Del Bene, J.S. Binkley, H.F. Schaefer III, J. Chem. Phys. 84 (1986) 2279.
[60] M. Trætteberg, H. Østensen, Acta Chem. Scand., Ser. A 33 (1979) 491.
[61] K.-M. Marstokk, H. Møllendal, Acta Chem. Scand., Ser. A 35 (1981) 395.
[62] J.M. Bakke, L.H. Bjerkeseth, J. Mol. Struct. 407 (1997) 27.
[63] P.J. Krueger, J. Jan, H. Wieser, J. Mol. Struct. 5 (1970) 375.
[64] M. Oki, H. Iwamura, Bull. Chem. Soc. Jpn. 32 (1959) 950.
[65] M. Oki, H. Iwamura, T. Onoda, M. Iwamura, Tetrahedron 24 (1968) 1905.
[66] J.M. Bakke, Acta Chem. Scand., Ser. B 40 (1986) 407.
[67] T. Zeegers-Huyskens, P. Huyskens, in: P.L. Huyskens, W.A.P. Luck, T. Zeegers-Huyskens (Eds.), Intermolecular Forces. An Introduction to Modern Methods and Results, Springer, Berlin, 1991 (Chapter 1).
[68] L. Pauling, The Nature of the Chemical Bond, 3rd ed., Cornell University Press, New York, 1960, p. 260.
[69] S. Scheiner, J. Mol. Struct. (Theochem) 202 (1989) 177.
[70] D. Feller, J. Chem. Phys. 96 (1992) 6104.
[71] D.W. Schwenke, D.G. Truhlar, J. Chem. Phys. 82 (1985) 2418.
[72] M. Gutowski, F.B. van Duijneveldt, G. Chalasinski, L. Piela, Mol. Phys. 61 (1987) 233.
[73] M. Gutowski, J.H. van Lenthe, J. Verbeek, F.B. van Duijneveldt, G. Chalasinski, Chem. Phys. Lett. 124 (1986) 370.
[74] F.B. van Duijneveldt, J.G.C.M. van Duijneveldt-van de Rijdt, J.H. van Lenthe, Chem. Rev. 94 (1994) 1873.
[75] J.J. Novoa, M. Planas, M.-H. Whangbo, J. Chem. Phys. Lett. 225 (1994) 240.
[76] S.K. Loushin, C.E. Dykstra, J. Comput. Chem. 8 (1987) 81.
[77] G. Chalasinski, M. Gutowski, Chem. Rev. 88 (1988) 943.
[78] A. Halkier, H. Koch, P. Jørgensen, O. Christiansen, I.M. Beck Nielsen, T. Helgeaker, Theor. Chem. Acc. 97 (1997) 150.
[79] A.K. Wilson, T. van Mourik, T.H. Dunning Jr., J. Mol. Struct. (Theochem) 388 (1996) 339.
[80] M.W. Feyereisen, D. Feller, D.A. Dixon, J. Phys. Chem. 100 (1996) 2993.
[81] W.J. Hehre, L. Radom, P.v.R. Schleyer, J.A. Pople, Ab Initio Molecular Orbital Theory, Wiley, New York, 1986.